Electronic Supplementary Material (ESI) for CrystEngComm.

Supplementary Information

Use of a Diels-Alder reaction to modify thermal expansion properties in charge-transfer cocrystals

Gary C. George III, Daniel K. Unruh, and Kristin M. Hutchins*

Department of Chemistry and Biochemistry, Texas Tech University, Lubbock, Texas, 79409, United States.

Email: kristin.hutchins@ttu.edu

1. Materials, Synthesis, and Crystallization

Materials

2,3-dichloromaleic anhydride (**DA1P**), thiourea, and 9-bromoanthracene (**BrAn**) were purchased from Oakwood Chemical. Allylamine was purchased from Arcos Organics. Magnesium sulfate, hexanes, chloroform, acetic acid, ethyl acetate, tetrahydrofuran (THF), and dichloromethane (DCM) were purchased from Fisher Chemical. Ethanol (200 proof) was purchased from Pharmco. All reagents were used as received.

Synthesis of DA1

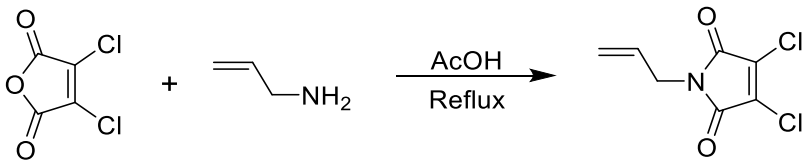

DA1P **DA1**

77 %

DA1 was synthesized following a previously reported synthesis.[1] In the first step, 1 g (6.0 mmol) of **DA1P** and 0.34 g (6.0 mmol) of allylamine were dissolved in THF (10 mL), and the THF was removed in vacuo. Next, 50 mL of glacial acetic acid was added to the mixture, which was then refluxed for 1.5 hours. The solvent was then removed in vacuo, and the resulting oil was refrigerated overnight, which allowed for crystallization of the crude product. The solid was then dissolved in DCM and purified via column chromatography, using an 80:20 mixture of hexane to ethyl acetate. The purified product weighed 0.9506 g, which resulted in a percent yield of 77%.

Synthesis of DA2

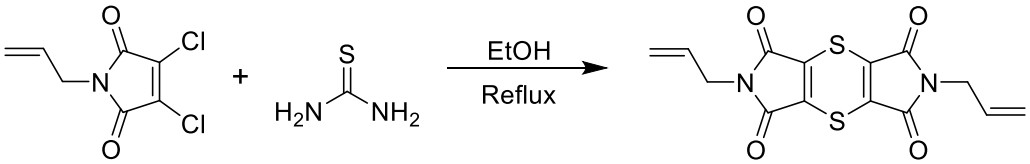

DA1 **DA2**

87 %

DA2 was synthesized following a previously reported synthesis.[1] In the first step, 0.200 g (0.97 mmol) of **DA1** was dissolved in ethanol (15 mL) in a 50 mL round bottom flask and heated to 80 °C. While heating, 0.074 g (0.97 mmol) of thiourea was added to a vial and

dissolved in ethanol (10 mL). The thiourea solution was added to the reaction flask, and the solution was refluxed for 2 hours. The reaction was cooled, the solvent was removed in vacuo, and the resulting green solid was dissolved in DCM and washed with water (20 mL portions, 3 times). A final washing was done with brine, followed by drying the organic layer with anhydrous magnesium sulfate. The organic layer was filtered and concentrated under vacuum, which gave 0.1421 g of **DA2**, resulting in a percent yield of 87%.

Crystallization of DA2-BrAn polymorphs. Single crystals were grown using two different methods, with each method giving a different proportion of each polymorph. Slow evaporation from a concentrated solution of DCM with 0.0150 g (0.045 mmol, 1 eq) of **DA2** and 0.0116 g (0.045 mmol, 1 eq) of **BrAn** over 2 days favored the head-to-head (H-H) polymorph. On the other hand, vapor diffusion with 0.0150 g (0.045 mmol, 1 eq) of **DA2** and 0.0116 g (0.045 mmol, 1 eq) of **BrAn** favored the head-to-tail (H-T) polymorph (see PXRD section). Vapor diffusion was conducted over a period of 2 days by dissolving both components in approximately 4 mL of DCM in an 8 mL vial, which was placed inside a 20 mL vial containing approximately 4 mL of hexanes. The H-T plates obtained from slow evaporation were smaller in size when compared to the vapor diffusion method.

Cycloaddition reactions. Cycloaddition reactions were conducted by placing the vials with crystals from either slow evaporation or vapor diffusion inside of an oven at 40-50 °C for ca. 1 month, or at 90-100 °C for a week.

Crystallization of DA2-BrAn Cycloadduct (CA) Nonsolvate. Single crystals were grown by dissolving approximately 0.0200 g of the reacted solid (mixture of H-H and H-T) in chloroform and allowing the solution to evaporate slowly over 3-4 days.

Crystallization of DA2-BrAn CA Solvate. Single crystals were grown by dissolving approximately 0.0200 g of the reacted solid (mixture of H-H and H-T) in DCM and allowing the solution to evaporate slowly over 2 days.

2. X-ray Diffraction Information and Data Tables

Data were collected on a Rigaku XtaLAB Synergy-*i*Kappa diffractometer equipped with a PhotonJet-*i* X-ray source operated at 50 W (50 kV, 1 mA) to generate Cu Kα radiation (λ = 1.54178 Å), or Mo Kα radiation (λ = 0.71073 Å) and a HyPix-6000HE HPC (hybrid photon counting) detector. Crystals were transferred from the vial and placed on a glass slide in type NVH immersion oil by Cargille. A Zeiss Stemi 305 microscope was used to identify a suitable specimen for X-ray diffraction from a representative sample of the material. The crystal and a small amount of the oil were collected on a Hampton Research 20 micron nylon loop, a 50 micron MiTeGen cryoloop, or a 200 micron MiTeGen cryoloop and transferred to the instrument where it was placed under a cold nitrogen stream (Oxford). Data were collected at temperatures from 100 K to 300 K in 20 K increments with a transition rate of 2 K/minute between the temperatures. The sample was optically centered with the aid of a video camera to ensure that no translations were observed as the crystal was rotated through all positions. The crystal was measured for size, morphology, and color.

After data collection, the unit cell was re-determined using a subset of the full data collection for each temperature. Intensity data were corrected for Lorentz, polarization, and background effects using *CrysAlis*^{Pro}.[2] A numerical absorption correction was applied based on a Gaussian integration over a multifaceted crystal and followed by a semi-empirical correction for adsorption applied using the program *SCALE3 ABSPACK*.[3] The program *SHELXT*[4] was used for the initial structure solution and SHELXL[5] was used for the refinement of the structures. Both of these programs were utilized within the OLEX2[6] software. Hydrogen atoms bound to carbon atoms were located in the difference Fourier map and were geometrically constrained using the appropriate AFIX commands.

In all four crystal structures, both of the allyl side chains are dynamically disordered at varying temperatures. These were modelled by splitting the respective carbons into parts (A and B) and letting each side chain freely refine independently. The refined occupancies of the A and B sites varied depending on temperature, and the two parts for each side chain were constrained to a total sum of one. To maintain reasonable bond lengths and ADPs for the disordered sites, RIGU, SIMU, and free variable DFIX restraints were applied where applicable. Hydrogen atoms bound to carbon atoms were geometrically constrained using the appropriate AFIX commands. In both cycloadducts, the bromine atom is positionally disordered through rotation of the molecule, with the disorder in the nonsolvate of 7%, and 5%

for the solvate structure. This was modelled using a free variable DFIX command. The nonsolvate cycloadduct exhibited disorder and showed larger thermal ellipsoids due to a static positional disorder of one of the sulfur atoms. This was modelled using a free variable DFIX command. Specifics about the disorder and modelling of these four structures can be found in the CIFs.

Table S1. X-ray data for **DA2-BrAn H-T** at 300, 280, 260, and 240 K.

compound formula	$C_{28}H_{19}BrN_2O_4S_2$	$C_{28}H_{19}BrN_2O_4S_2$	$C_{28}H_{19}BrN_2O_4S_2$	$C_{28}H_{19}BrN_2O_4S_2$
formula mass	591.48	591.48	591.48	591.48
crystal system	monoclinic	monoclinic	monoclinic	monoclinic
space group	*P2₁/n*	*P2₁/n*	*P2₁/n*	*P2₁/n*
a/Å	12.8724(2)	12.8651(3)	12.86180(10)	12.85730(10)
b/Å	13.7868(3)	13.7494(3)	13.7157(2)	13.6803(2)
c/Å	14.7545(3)	14.7302(4)	14.7240(2)	14.7126(2)
α/°	90	90	90	90
β/°	107.441(2)	107.516(2)	107.5340(10)	107.5780(10)
γ/°	90	90	90	90
V/Å^3	2498.09(9)	2484.77(11)	2476.76(5)	2466.99(5)
ρ_{calc}/g cm^{-3}	1.573	1.581	1.586	1.593
T/K	300.05(10)	280.05(10)	260.06(10)	240.05(10)
Z	4	4	4	4
radiation type	CuKα	CuKα	CuKα	CuKα
absorption coefficient, μ/mm^{-1}	4.136	4.158	4.172	4.188
crystal size/mm^3	0.233 × 0.157 × 0.103	0.233 × 0.157 × 0.103	0.233 × 0.157 × 0.103	0.233 × 0.157 × 0.103
no. of reflections measured	42660	41163	44913	46163
no. of independent reflections	5142	5163	5153	5132
no. of reflections (I > 2σ(I))	4048	4187	4326	4387
R_{int}	0.0566	0.0556	0.0501	0.0484
R_1 (I > 2σ(I))	0.0314	0.0316	0.0284	0.0277
$wR(F^2)$ (I > 2σ(I))	0.0777	0.0812	0.0745	0.0720
R_1 (all data)	0.0457	0.0426	0.0369	0.0349
$wR(F^2)$ (all data)	0.0915	0.0911	0.0823	0.0792

Goodness-of-fit	1.045	1.038	1.054	1.012
CCDC deposition number	2179716	2179715	2179714	2179713

Table S2. X-ray data for **DA2-BrAn H-T** at 220, 200, 180, and 160 K.

compound formula	$C_{28}H_{19}BrN_2O_4S_2$	$C_{28}H_{19}BrN_2O_4S_2$	$C_{28}H_{19}BrN_2O_4S_2$	$C_{28}H_{19}BrN_2O_4S_2$
formula mass	591.48	591.48	591.48	591.48
crystal system	monoclinic	monoclinic	monoclinic	monoclinic
space group	*P2₁/n*	*P2₁/n*	*P2₁/n*	*P2₁/n*
a/Å	12.85490(10)	12.85220(10)	12.85000(10)	12.84750(10)
b/Å	13.64830(10)	13.6143(2)	13.58420(10)	13.55560(10)
c/Å	14.70060(10)	14.6879(2)	14.6753(2)	14.6645(2)
α/°	90	90	90	90
β/°	107.6290(10)	107.6790(10)	107.7230(10)	107.7640(10)
γ/°	90	90	90	90
V/Å^3	2458.06(3)	2448.62(5)	2440.10(4)	2432.14(4)
ρ_{calc}/g cm^{-3}	1.598	1.604	1.610	1.615
T/K	220.05(10)	200.05(10)	180.06(10)	160.06(10)
Z	4	4	4	4
radiation type	CuKα	CuKα	CuKα	CuKα
absorption coefficient, μ/mm^{-1}	4.204	4.220	4.235	4.248
crystal size/mm^3	0.233 × 0.157 × 0.103	0.233 × 0.157 × 0.103	0.233 × 0.157 × 0.103	0.233 × 0.157 × 0.107
no. of reflections measured	46057	45046	44835	45208
no. of independent reflections	5123	5108	5089	5086
no. of reflections (I > 2σ(I))	4462	4517	4562	4616
R_{int}	0.0477	0.0443	0.0421	0.0422
R_1 (I > 2σ(I))	0.0274	0.0258	0.0278	0.0266
$wR(F^2)$ (I > 2σ(I))	0.0710	0.0674	0.0731	0.0710
R_1 (all data)	0.0335	0.0310	0.0324	0.0303
$wR(F^2)$ (all data)	0.0774	0.0725	0.0780	0.0747
Goodness-of-fit	1.040	1.052	1.049	1.040
CCDC deposition number	2179712	2179711	2179710	2179709

Table S3. X-ray data for **DA2-BrAn H-T** at 140, 120, and 100 K.

compound formula	$C_{28}H_{19}BrN_2O_4S_2$	$C_{28}H_{19}BrN_2O_4S_2$	$C_{28}H_{19}BrN_2O_4S_2$
formula mass	591.48	591.48	591.48
crystal system	monoclinic	monoclinic	monoclinic
space group	*P2₁/n*	*P2₁/n*	*P2₁/n*
a/Å	12.84410(10)	12.84010(10)	12.8343(2)
b/Å	13.53080(10)	13.50710(10)	13.4844(2)
c/Å	14.6539(2)	14.6451(2)	14.6371(2)
α/°	90	90	90
β/°	107.8020(10)	107.8340(10)	107.8630(10)
γ/°	90	90	90
V/Å^3	2424.77(4)	2417.89(4)	2411.02(6)
ρ_{calc}/g cm^{-3}	1.620	1.625	1.629
T/K	140.05(10)	120.03(12)	99.9(4)
Z	4	4	4
radiation type	CuKα	CuKα	CuKα
absorption coefficient, μ/mm^{-1}	4.261	4.273	4.286
crystal size/mm^3	0.233 × 0.157 × 0.103	0.233 × 0.157 × 0.103	0.233 × 0.157 × 0.103
no. of reflections measured	44828	44635	44546
no. of independent reflections	5075	5072	5042
no. of reflections (I > 2σ(I))	4663	4695	4728
R_{int}	0.0417	0.0409	0.0414
R_1 (I > 2σ(I))	0.0266	0.0260	0.0266
$wR(F^2)$ (I > 2σ(I))	0.0711	0.0706	0.0707
R_1 (all data)	0.0295	0.0287	0.0288
$wR(F^2)$ (all data)	0.0741	0.0733	0.0729
Goodness-of-fit	1.053	1.063	1.064
CCDC deposition number	2179708	2179707	2179706

Table S4. X-ray data for **DA2-BrAn H-H** at 300, 280, 260, and 240 K.

compound formula	$C_{28}H_{19}BrN_2O_4S_2$	$C_{28}H_{19}BrN_2O_4S_2$	$C_{28}H_{19}BrN_2O_4S_2$	$C_{28}H_{19}BrN_2O_4S_2$
formula mass	591.48	591.48	591.48	591.48
crystal system	triclinic	triclinic	triclinic	triclinic
space group	*P-1*	*P-1*	*P-1*	*P-1*
a/Å	7.36340(10)	7.34440(10)	7.32560(10)	7.30960(10)
b/Å	10.50400(10)	10.50070(10)	10.50030(10)	10.49630(10)
c/Å	17.22370(10)	17.20520(10)	17.18510(10)	17.16230(10)
α/°	74.3220(10)	74.2550(10)	74.1950(10)	74.1460(10)
β/°	83.2550(10)	83.3210(10)	83.4010(10)	83.4770(10)
γ/°	86.4410(10)	86.4110(10)	86.3720(10)	86.3390(10)
V/Å^3	1273.09(2)	1267.77(2)	1262.79(2)	1257.73(2)
ρ_{calc}/g cm^{-3}	1.543	1.549	1.556	1.562
T/K	300.05(10)	280.04(10)	260.04(10)	240.04(10)
Z	2	2	2	2
radiation type	CuKα	CuKα	CuKα	CuKα
absorption coefficient, μ/mm^{-1}	4.058	4.075	4.091	4.108
crystal size/mm^3	0.157 × 0.07 × 0.049	0.157 × 0.07 × 0.049	0.157 × 0.07 × 0.049	0.157 × 0.07 × 0.049
no. of reflections measured	42812	44209	44135	45148
no. of independent reflections	4537	4537	4517	4498
no. of reflections (I > 2σ(I))	3920	3988	4048	4079
R_{int}	0.0511	0.0519	0.0488	0.0478
R_1 (I > 2σ(I))	0.0329	0.0315	0.0306	0.0295
$wR(F^2)$ (I > 2σ(I))	0.0856	0.0824	0.0803	0.0777
R_1 (all data)	0.0396	0.0371	0.0346	0.0337
$wR(F^2)$ (all data)	0.0912	0.0872	0.0830	0.0815
Goodness-of-fit	1.034	1.027	1.035	1.035
CCDC deposition number	2179705	2179704	2179703	2179702

Table S5. X-ray data for **DA2-BrAn H-H** at 220, 200, 180, and 160 K.

compound formula	$C_{28}H_{19}BrN_2O_4S_2$	$C_{28}H_{19}BrN_2O_4S_2$	$C_{28}H_{19}BrN_2O_4S_2$	$C_{28}H_{19}BrN_2O_4S_2$
formula mass	591.48	591.48	591.48	591.48
crystal system	triclinic	triclinic	triclinic	triclinic
space group	*P-1*	*P-1*	*P-1*	*P-1*
a/Å	7.29340(10)	7.27770(10)	7.26160(10)	7.24750(10)
b/Å	10.49260(10)	10.4880(2)	10.48750(10)	10.48160(10)
c/Å	17.1456(2)	17.1243(3)	17.0975(2)	17.0769(2)
α/°	74.0890(10)	74.082(2)	74.0600(10)	74.0430(10)
β/°	83.5460(10)	83.614(2)	83.7520(10)	83.8400(10)
γ/°	86.3150(10)	86.328(2)	86.2640(10)	86.2470(10)
V/Å^3	1253.06(3)	1248.38(4)	1243.73(3)	1239.19(3)
ρ_{calc}/g cm^{-3}	1.568	1.574	1.579	1.585
T/K	220.01(10)	200.00(10)	180.05(10)	160.05(10)
Z	2	2	2	2
radiation type	CuKα	CuKα	CuKα	CuKα
absorption coefficient, μ/mm^{-1}	4.123	4.138	4.154	4.169
crystal size/mm^3	0.157 × 0.07 × 0.049	0.157 × 0.07 × 0.049	0.157 × 0.07 × 0.049	0.157 × 0.07 × 0.049
no. of reflections measured	44408	43781	44948	45509
no. of independent reflections	4477	4453	5151	5131
no. of reflections (I > 2σ(I))	4100	4082	4675	4722
R_{int}	0.0464	0.0479	0.0477	0.0479
R_1 (I > 2σ(I))	0.0291	0.0293	0.0353	0.0352
$wR(F^2)$ (I > 2σ(I))	0.0758	0.0761	0.0909	0.0908
R_1 (all data)	0.0321	0.0324	0.0387	0.0381
$wR(F^2)$ (all data)	0.0781	0.0783	0.0931	0.0928
Goodness-of-fit	1.019	1.036	1.063	1.075
CCDC deposition number	2179701	2179700	2179699	2179698

Table S6. X-ray data for **DA2-BrAn H-H** at 140, 120, and 100 K.

compound formula	$C_{28}H_{19}BrN_2O_4S_2$	$C_{28}H_{19}BrN_2O_4S_2$	$C_{28}H_{19}BrN_2O_4S_2$
formula mass	591.48	591.48	591.48
crystal system	triclinic	triclinic	triclinic
space group	*P-1*	*P-1*	*P-1*
a/Å	7.23490(10)	7.22410(10)	7.21410(10)
b/Å	10.47620(10)	10.4714(2)	10.4674(2)
c/Å	17.0549(2)	17.0316(3)	17.0117(3)
α/°	74.0330(10)	74.0370(10)	74.024(2)
β/°	83.9240(10)	83.9990(10)	84.049(2)
γ/°	86.2310(10)	86.2270(10)	86.219(2)
V/Å^3	1234.90(3)	1230.99(4)	1227.39(4)
ρ_{calc}/g cm^{-3}	1.591	1.596	1.600
T/K	140.06(10)	120.02(11)	99.97(15)
Z	2	2	2
radiation type	CuKα	CuKα	CuKα
absorption coefficient, μ/mm^{-1}	4.184	4.197	4.209
crystal size/mm^3	0.157 × 0.07 × 0.049	0.157 × 0.07 × 0.049	0.157 × 0.07 × 0.049
no. of reflections measured	45013	42486	40991
no. of independent reflections	5099	4390	4375
no. of reflections ($I > 2\sigma(I)$)	4723	4146	4124
R_{int}	0.0463	0.0475	0.0483
R_1 ($I > 2\sigma(I)$)	0.0344	0.0301	0.0300
$wR(F^2)$ ($I > 2\sigma(I)$)	0.0884	0.0797	0.0783
R_1 (all data)	0.0369	0.0319	0.0317
$wR(F^2)$ (all data)	0.0899	0.0809	0.0793
Goodness-of-fit	1.091	1.050	1.046
CCDC deposition number	2179697	2179696	2179695

Table S7. X-ray data for **DA2-BrAn CA Nonsolvate** at 300, 280, 260, and 240 K.

compound formula	$C_{28}H_{19}BrN_2O_4S_2$	$C_{28}H_{19}BrN_2O_4S_2$	$C_{28}H_{19}BrN_2O_4S_2$	$C_{28}H_{19}BrN_2O_4S_2$
formula mass	591.48	591.48	591.48	591.48
crystal system	monoclinic	monoclinic	monoclinic	monoclinic
space group	$P2_1/n$	$P2_1/n$	$P2_1/n$	$P2_1/n$
a/Å	12.8827(2)	12.8422(2)	12.8024(2)	12.7684(2)
b/Å	23.1663(3)	23.1663(3)	23.1655(2)	23.1636(3)
c/Å	8.5489(2)	8.53950(10)	8.53020(10)	8.52030(10)
α/°	90	90	90	90
β/°	102.983(2)	102.991(2)	102.9910(10)	102.974(2)
γ/°	90	90	90	90
V/Å^3	2486.15(8)	2475.53(6)	2465.08(5)	2455.65(6)
ρ_{calc}/g cm^{-3}	1.580	1.587	1.594	1.600
T/K	300.06(10)	280.06(10)	260.05(10)	240.05(10)
Z	4	4	4	4
radiation type	CuKα	CuKα	CuKα	CuKα
absorption coefficient, μ/mm^{-1}	4.156	4.174	4.192	4.208
crystal size/mm^3	0.187 × 0.099 × 0.044	0.187 × 0.099 × 0.044	0.187 × 0.099 × 0.044	0.187 × 0.099 × 0.044
no. of reflections measured	33327	32756	34642	34959
no. of independent reflections	5028	5003	5033	5040
no. of reflections (I > 2σ(I))	3978	4111	4246	4373
R_{int}	0.0760	0.0736	0.0689	0.0691
R_1 (I > 2σ(I))	0.0457	0.0464	0.0445	0.0450
wR(F^2) (I > 2σ(I))	0.1088	0.1062	0.1022	0.1019
R_1 (all data)	0.0593	0.0575	0.0537	0.0526
wR(F^2) (all data)	0.1167	0.1123	0.1076	0.1059
Goodness-of-fit	1.049	1.048	1.059	1.055
CCDC deposition number	2179683	2179682	2179681	2179680

Table S8. X-ray data for **DA2-BrAn CA Nonsolvate** at 220, 200, 180, and 160 K.

compound formula	$C_{28}H_{19}BrN_2O_4S_2$	$C_{28}H_{19}BrN_2O_4S_2$	$C_{28}H_{19}BrN_2O_4S_2$	$C_{28}H_{19}BrN_2O_4S_2$
formula mass	591.48	591.48	591.48	591.48
crystal system	monoclinic	monoclinic	monoclinic	monoclinic
space group	*P2₁/n*	*P2₁/n*	*P2₁/n*	*P2₁/n*
a/Å	12.7367(2)	12.7092(2)	12.68870(10)	12.6761(2)
b/Å	23.1582(3)	23.1518(3)	23.1336(2)	23.1148(3)
c/Å	8.51220(10)	8.50430(10)	8.49540(10)	8.48800(10)
α/°	90	90	90	90
β/°	102.958(2)	102.9460(10)	102.9400(10)	102.9490(10)
γ/°	90	90	90	90
V/Å^3	2446.81(6)	2438.71(6)	2430.37(4)	2423.78(6)
ρ_{calc}/g cm^{-3}	1.606	1.611	1.617	1.621
T/K	220.05(10)	200.05(10)	180.05(10)	160.04(10)
Z	4	4	4	4
radiation type	CuKα	CuKα	CuKα	CuKα
absorption coefficient, μ/mm^{-1}	4.223	4.237	4.251	4.263
crystal size/mm^3	0.187 × 0.099 × 0.044	0.187 × 0.099 × 0.044	0.187 × 0.099 × 0.044	0.187 × 0.099 × 0.044
no. of reflections measured	35645	37025	40373	46027
no. of independent reflections	5048	5049	5050	5012
no. of reflections (I > 2σ(I))	4464	4562	4650	4684
R_{int}	0.0712	0.0735	0.0686	0.0634
R_1 (I > 2σ(I))	0.0443	0.0449	0.0426	0.0414
$wR(F^2)$ (I > 2σ(I))	0.1009	0.0993	0.0947	0.0888
R_1 (all data)	0.0500	0.0493	0.0464	0.0442
$wR(F^2)$ (all data)	0.1035	0.1014	0.0967	0.0902
Goodness-of-fit	1.080	1.087	1.116	1.135
CCDC deposition number	2179679	2179678	2179677	2179676

Table S9. X-ray data for **DA2-BrAn CA Nonsolvate** at 140, 120, and 100 K.

compound formula	$C_{28}H_{19}BrN_2O_4S_2$	$C_{28}H_{19}BrN_2O_4S_2$	$C_{28}H_{19}BrN_2O_4S_2$
formula mass	591.48	591.48	591.48
crystal system	monoclinic	monoclinic	monoclinic
space group	*P2₁/n*	*P2₁/n*	*P2₁/n*
a/Å	12.66500(10)	12.65620(10)	12.6484(2)
b/Å	23.0937(2)	23.0704(2)	23.0505(2)
c/Å	8.48130(10)	8.47410(10)	8.46750(10)
α/°	90	90	90
β/°	102.9490(10)	102.9600(10)	102.9730(10)
γ/°	90	90	90
V/Å^3	2417.54(4)	2411.27(4)	2405.70(5)
ρ_{calc}/g cm^{-3}	1.625	1.629	1.633
T/K	140.05(10)	120.02(15)	100.01(10)
Z	4	4	4
radiation type	CuKα	CuKα	CuKα
absorption coefficient, μ/mm^{-1}	4.274	4.285	4.295
crystal size/mm^3	0.187 × 0.099 × 0.044	0.187 × 0.099 × 0.044	0.187 × 0.099 × 0.044
no. of reflections measured	44489	48441	49733
no. of independent reflections	4986	4988	4989
no. of reflections (I > 2σ(I))	4702	4760	4759
R_{int}	0.0562	0.0557	0.0551
R_1 (I > 2σ(I))	0.0410	0.0409	0.0409
$wR(F^2)$ (I > 2σ(I))	0.0858	0.0835	0.0841
R_1 (all data)	0.0434	0.0429	0.0428
$wR(F^2)$ (all data)	0.0869	0.0844	0.0850
Goodness-of-fit	1.142	1.154	1.168
CCDC deposition number	2179675	2179674	2179673

Table S10. X-ray data for **DA2-BrAn H-T CA Solvate** at 300, 280, 260, and 240 K.

compound formula	$C_{29}H_{21}BrCl_2N_2O_4S_2$	$C_{29}H_{21}BrCl_2N_2O_4S_2$	$C_{29}H_{21}BrCl_2N_2O_4S_2$	$C_{29}H_{21}BrCl_2N_2O_4S_2$
formula mass	676.41	676.41	676.41	676.41
crystal system	triclinic	triclinic	triclinic	triclinic
space group	*P-1*	*P-1*	*P-1*	*P-1*
a/Å	8.30080(10)	8.28710(10)	8.27430(10)	8.26160(10)
b/Å	12.6587(2)	12.6405(2)	12.6240(2)	12.6082(2)
c/Å	14.6123(3)	14.5859(3)	14.5612(3)	14.5375(2)
α/°	110.224(2)	110.159(2)	110.093(2)	110.024(2)
β/°	90.1780(10)	90.2630(10)	90.3500(10)	90.4470(10)
γ/°	100.2070(10)	100.1920(10)	100.1880(10)	100.1750(10)
V/Å^3	1414.51(4)	1408.12(4)	1402.21(4)	1396.54(4)
ρ_{calc}/g cm^{-3}	1.588	1.595	1.602	1.609
T/K	300.06(10)	280.05(10)	260.05(10)	240.05(10)
Z	2	2	2	2
radiation type	CuKα	CuKα	CuKα	CuKα
absorption coefficient, μ/mm^{-1}	5.430	5.454	5.477	5.500
crystal size/mm^3	0.22 × 0.131 × 0.098	0.22 × 0.131 × 0.098	0.22 × 0.131 × 0.098	0.22 × 0.131 × 0.098
no. of reflections measured	25740	26444	24644	25394
no. of independent reflections	5794	5780	5746	5723
no. of reflections (I > 2σ(I))	4528	4658	4721	4825
R_{int}	0.0627	0.0618	0.0581	0.0590
R_1 (I > 2σ(I))	0.0451	0.0438	0.0419	0.0408
$wR(F^2)$ (I > 2σ(I))	0.1139	0.1105	0.1047	0.1031
R_1 (all data)	0.0575	0.0544	0.0517	0.0482
$wR(F^2)$ (all data)	0.1253	0.1209	0.1141	0.1096
Goodness-of-fit	1.060	1.038	1.031	1.054
CCDC deposition number	2179694	2179693	2179692	2179691

Table S11. X-ray data for **DA2-BrAn H-T CA Solvate** at 220, 200, 180, and 160 K.

compound formula	$C_{29}H_{21}BrCl_2N_2O_4S_2$	$C_{29}H_{21}BrCl_2N_2O_4S_2$	$C_{29}H_{21}BrCl_2N_2O_4S_2$	$C_{29}H_{21}BrCl_2N_2O_4S_2$
formula mass	676.41	676.41	676.41	676.41
crystal system	triclinic	triclinic	triclinic	triclinic
space group	*P-1*	*P-1*	*P-1*	*P-1*
a/Å	8.24900(10)	8.23820(10)	8.22720(10)	8.21730(10)
b/Å	12.5938(2)	12.5766(2)	12.5614(2)	12.5465(2)
c/Å	14.5158(2)	14.4942(2)	14.4730(2)	14.4534(2)
α/°	109.9650(10)	109.9020(10)	109.8260(10)	109.7610(10)
β/°	90.5380(10)	90.6370(10)	90.7290(10)	90.8080(10)
γ/°	100.1680(10)	100.1610(10)	100.1510(10)	100.1480(10)
V/Å^3	1391.14(4)	1385.77(3)	1380.78(3)	1376.06(3)
ρ_{calc}/g cm^{-3}	1.615	1.621	1.627	1.632
T/K	220.06(10)	200.05(10)	180.05(10)	160.06(10)
Z	2	2	2	2
radiation type	CuKα	CuKα	CuKα	CuKα
absorption coefficient, μ/mm^{-1}	5.521	5.542	5.562	5.582
crystal size/mm^3	0.22 × 0.131 × 0.098	0.22 × 0.131 × 0.098	0.22 × 0.131 × 0.098	0.22 × 0.131 × 0.098
no. of reflections measured	25784	26210	24300	24568
no. of independent reflections	5700	5690	5623	5615
no. of reflections (I > 2σ(I))	4876	4996	5025	5055
R_{int}	0.0572	0.0557	0.0513	0.0514
R_1 (I > 2σ(I))	0.0387	0.0369	0.0365	0.0352
$wR(F^2)$ (I > 2σ(I))	0.0987	0.0934	0.0912	0.0883
R_1 (all data)	0.0453	0.0422	0.0410	0.0392
$wR(F^2)$ (all data)	0.1042	0.0981	0.0957	0.0922
Goodness-of-fit	1.061	1.051	1.057	1.055
CCDC deposition number	2179690	2179689	2179688	2179687

Table S12. X-ray data for **DA2-BrAn H-T CA Solvate** at 140, 120, and 100 K.

compound formula	$C_{29}H_{21}BrCl_2N_2O_4S_2$	$C_{29}H_{21}BrCl_2N_2O_4S_2$	$C_{29}H_{21}BrCl_2N_2O_4S_2$
formula mass	676.41	676.41	676.41
crystal system	triclinic	triclinic	triclinic
space group	*P-1*	*P-1*	*P-1*
a/Å	8.20890(10)	8.20170(10)	8.19530(10)
b/Å	12.5322(2)	12.5179(2)	12.5048(2)
c/Å	14.4357(2)	14.4178(2)	14.4006(2)
α/°	109.7000(10)	109.6400(10)	109.5920(10)
β/°	90.8830(10)	90.9480(10)	91.0160(10)
γ/°	100.1350(10)	100.1250(10)	100.1160(10)
V/Å^3	1371.86(3)	1367.85(3)	1364.05(3)
ρ_{calc}/g cm^{-3}	1.637	1.642	1.647
T/K	140.05(10)	120.05(10)	99.99(16)
Z	2	2	2
radiation type	CuKα	CuKα	CuKα
absorption coefficient, μ/mm^{-1}	5.599	5.615	5.631
crystal size/mm^3	0.22 × 0.131 × 0.098	0.22 × 0.131 × 0.098	0.22 × 0.131 × 0.098
no. of reflections measured	25006	25222	25558
no. of independent reflections	5641	5619	5627
no. of reflections (I > 2σ(I))	5137	5185	5241
R_{int}	0.0507	0.0504	0.0489
R_1 (I > 2σ(I))	0.0340	0.0338	0.0336
$wR(F^2)$ (I > 2σ(I))	0.0836	0.0844	0.0856
R_1 (all data)	0.0374	0.0366	0.0364
$wR(F^2)$ (all data)	0.0870	0.0868	0.0888
Goodness-of-fit	1.036	1.061	1.080
CCDC deposition number	2179686	2179685	2179684

Table S13. X-ray data for **DA2-BrAn CAs** (non-solvate and solvate) obtained from recrystallization of the H-H reacted product at 100 K.

compound formula	$C_{28}H_{19}BrN_2O_4S_2$	$C_{29}H_{21}BrCl_2N_2O_4S_2$
formula mass	591.48	676.41
crystal system	Monoclinic	Triclinic
space group	*P2₁/c*	*P-1*
a/Å	12.6744(2)	8.20200(10)
b/Å	23.0269(3)	12.5063(2)
c/Å	8.48040(10)	14.4204(2)
α/°	90	109.6660(10)
β/°	103.198(2)	90.9300(10)
γ/°	90	100.1330(10)
V/Å^3	2409.65(6)	1366.64(3)
ρ_{calc}/g cm^{-3}	1.630	1.644
T/K	100.00(10)	100.00(10)
Z	4	2
radiation type	CuKα	CuKα
absorption coefficient, μ/mm^{-1}	4.288	5.620
crystal size/mm^3	0.267 x 0.149 x 0.039	0.255 x 0.09 x 0.037
no. of reflections measured	26084	28767
no. of independent reflections	4944	5525
no. of reflections (I > 2σ(I))	4469	5031
R_{int}	0.0638	0.0668
R_1 (I > 2σ(I))	0.0624	0.0416
wR(F^2) (I > 2σ(I))	0.1329	0.1073
R_1 (all data)	0.0681	0.0450
wR(F^2) (all data)	0.1360	0.1096
Goodness-of-fit	1.108	1.057
CCDC deposition number	2179671	2179672

3. Thermal Expansion Data and Intermolecular Interaction Distances

The TE coefficients were calculated using the PASCal program.[7] The unit cell parameters from the crystallographic data sets collected from 100-300 K were used for the TE calculations.

Table S14. TE coefficients for the crystals. Errors are denoted in parentheses and approximate crystallographic axes are denoted in brackets.

Crystal	α_{X_1} (MK^{-1}) [axis]	α_{X_2} (MK^{-1}) [axis]	α_{X_3}(MK^{-1}) [axis]	α_V(MK^{-1})
DA2-BrAn H-T	8 (1) [3 0 -1]	56 (2) [3 0 4]	113 (3) [0 1 0]	179 (5)
DA2-BrAn H-H	17 (1) [2 5 -1]	38 (1) [-4 1 2]	130 (3) [5 -1 2]	188 (3)
DA2-BrAn H-T CA Non-solvate	28 (3) [1 0 -5]	47 (1) [0 -1 0]	90 (8) [4 0 3]	168 (6)
DA2-BrAn H-T CA Solvate	16 (1) [-1 1 1]	58 (2) [1 1 0]	109 (3) [4 -1 3]	186 (5)

Table S15. Intermolecular interaction distances.

Crystal	C-H···O (Å) 300 K	C-H···O (Å) 100 K	Δ (Å)
DA2-BrAn H-T	3.378 3.436 3.288 3.373 3.638	3.339 3.357 3.224 3.318 3.593	0.039 0.079 0.064 0.055 0.045 Avg: 0.056
DA2-BrAn H-H	3.609 3.359 3.344 3.450 3.744 3.553 3.336	3.517 3.284 3.301 3.375 3.616 3.504 3.272	0.092 0.075 0.043 0.075 0.128 0.049 0.064 Avg: 0.075
DA2-BrAn H-T CA Non-solvate	3.399 3.373 3.197 3.063 3.410 3.596 3.317	3.265 3.252 3.140 3.012 3.323 3.550 3.245	0.134 0.121 0.057 0.051 0.087 0.046 0.072 Avg: 0.081

DA2-BrAn H-T CA Solvate	3.535 3.562 3.771 3.203 3.473	3.390 3.468 3.602 3.211 3.379	0.145 0.094 0.169 -0.008 0.094 Avg: 0.099

Crystal	π··· π (Å) 300 K	π ··· π (Å) 100 K	Δ (Å)
DA2-BrAn H-T	3.453 3.476 3.481 3.430	3.373 3.393 3.398 3.347	0.080 0.084 0.082 0.083 Avg: 0.082
DA2-BrAn H-H	3.940 3.607 3.467 3.440 3.388 3.549 3.567 3.463 3.412 3.454 3.472	3.777 3.490 3.389 3.378 3.319 3.481 3.505 3.371 3.342 3.389 3.398	0.163 0.117 0.078 0.062 0.069 0.068 0.062 0.092 0.070 0.065 0.074 Avg: 0.084
DA2-BrAn H-T CA Non-solvate	N/A	N/A	N/A
DA2-BrAn H-T CA Solvate	3.661	3.572	0.089

Crystal	C-H···S (Å) 300 K	C-H···S (Å) 100 K	Δ (Å)
DA2-BrAn H-T	3.763	3.735	0.028
DA2-BrAn H-H	3.729	3.692	0.037
DA2-BrAn H-T CA Non-solvate	N/A	N/A	N/A
DA2-BrAn H-T CA Solvate	3.818 3.880	3.771 3.877	0.051 0.003

Crystal	C-H···π (Å) 300 K	C-H···π (Å) 100 K	Δ (Å)
DA2-BrAn H-T	3.788 3.701 3.929 3.450	3.675 3.612 3.742 3.390	0.113 0.089 0.187 0.060
DA2-BrAn H-H	N/A	N/A	N/A

DA2-BrAn H-T CA Non-solvate	3.853 3.955	3.787 3.837	0.066 0.118
DA2-BrAn H-T CA Solvate	3.869 3.870 3.615 3.621	3.838 3.824 3.543 3.574	0.031 0.046 0.072 0.047

Crystal	allyl···allyl (Å) 300 K	allyl···allyl (Å) 100 K	Δ (Å)
DA2-BrAn H-T	N/A	N/A	N/A
DA2-BrAn H-H	N/A	N/A	N/A
DA2-BrAn H-T CA Non-solvate	3.801 3.765 3.842	3.654 3.736 3.742	0.147 0.029 0.100
DA2-BrAn H-T CA Solvate	4.301	4.182	0.119

Crystal	S···S (Å) 300 K	S···S (Å) 100 K	Δ (Å)
DA2-BrAn H-T	N/A	N/A	N/A
DA2-BrAn H-H	N/A	N/A	N/A
DA2-BrAn H-T CA Non-solvate	3.681	3.652	0.029
DA2-BrAn H-T CA Solvate	3.548	3.416	0.132

Crystal	Br···π (Å) 300 K	Br···π (Å) 100 K	Δ (Å)
DA2-BrAn H-T	N/A	N/A	N/A
DA2-BrAn H-H	N/A	N/A	N/A
DA2-BrAn H-T CA Non-solvate	3.654	3.537	0.117
DA2-BrAn H-T CA Solvate	3.844 3.833	3.716 3.735	0.128 0.098

4. Expansivity Indicatrix Diagrams

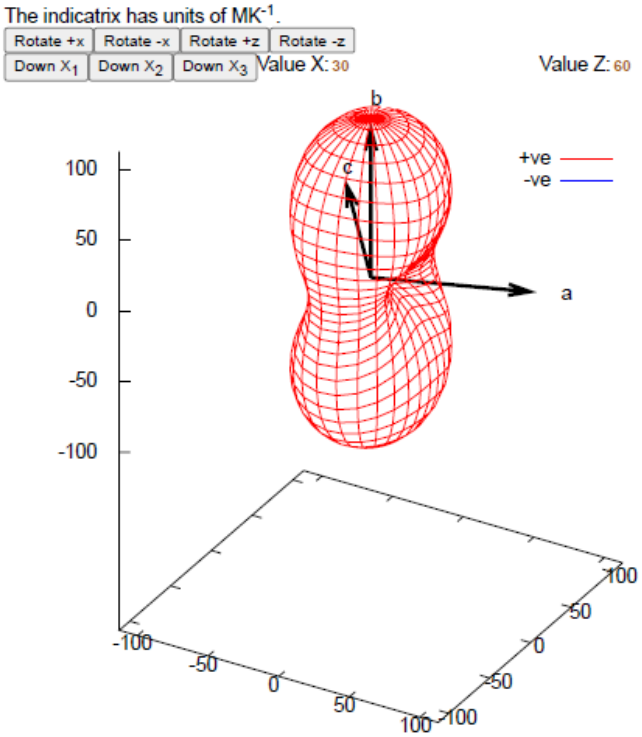

Figure S1. Thermal expansivity indicatrix for **DA2-BrAn H-T**.

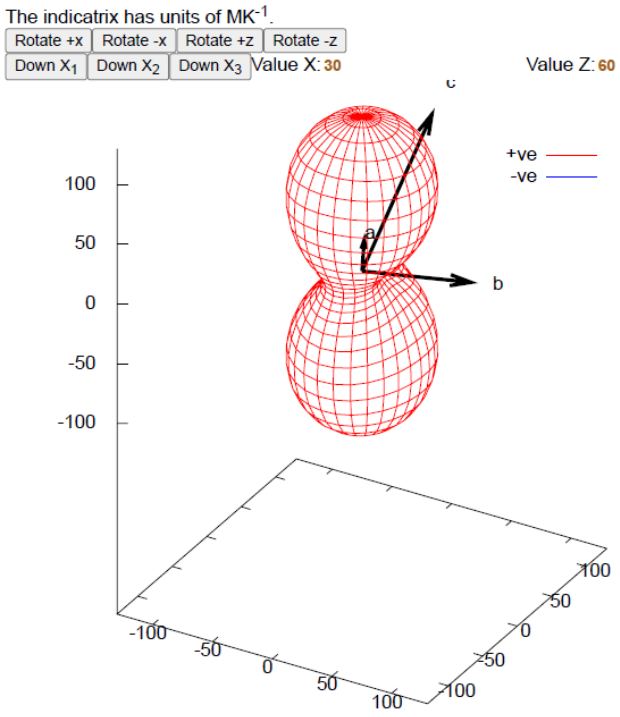

Figure S2. Thermal expansivity indicatrix for **DA2-BrAn H-H**.

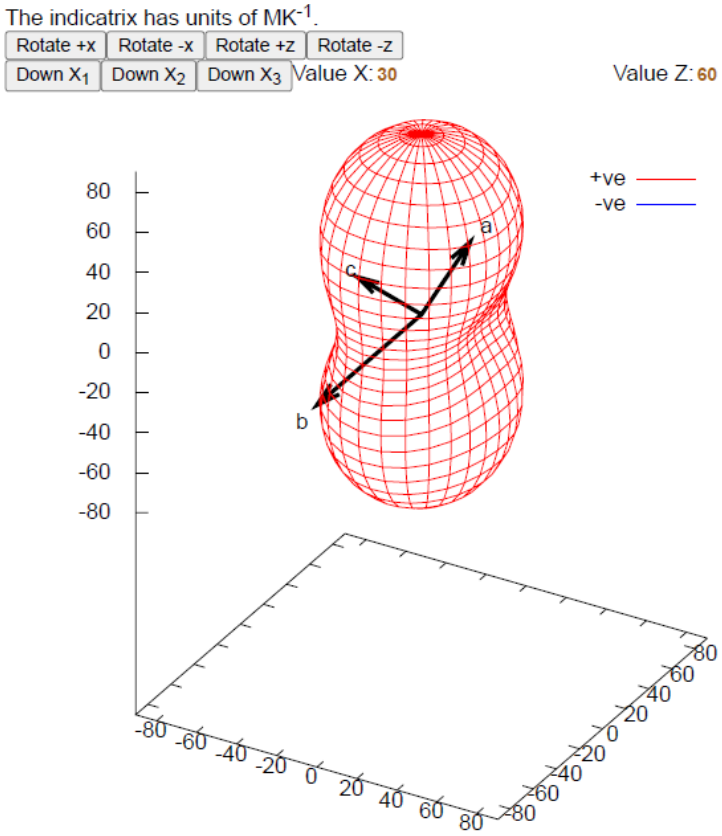

Figure S3. Thermal expansivity indicatrix for **DA2-BrAn CA Nonsolvate**.

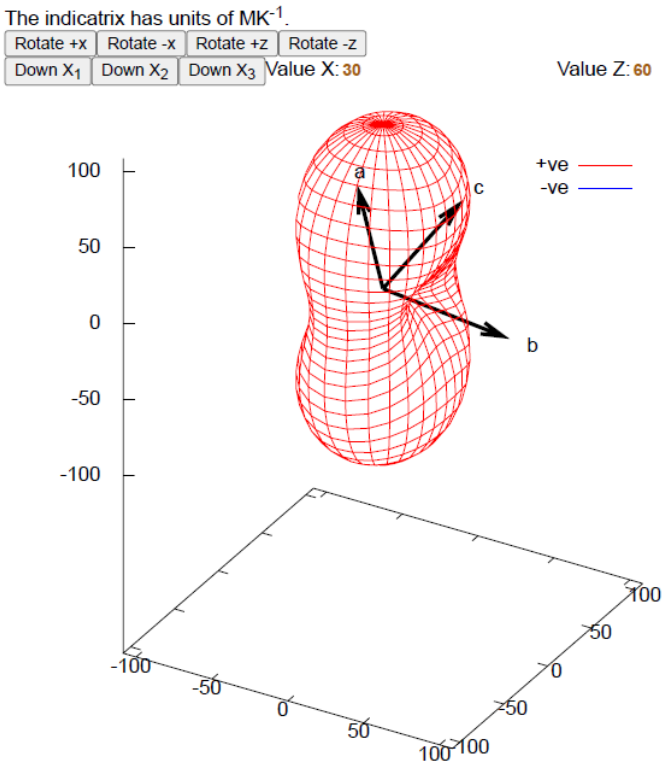

Figure S4. Thermal expansivity indicatrix for **DA2-BrAn CA Solvate**.

5. NMR Spectra of the Compounds

All the compounds were dissolved in $CDCl_3$ or DMSO-d_6 for NMR experiments. NMR data was collected using a JOEL ECS 400 MHZ Spectrometer.

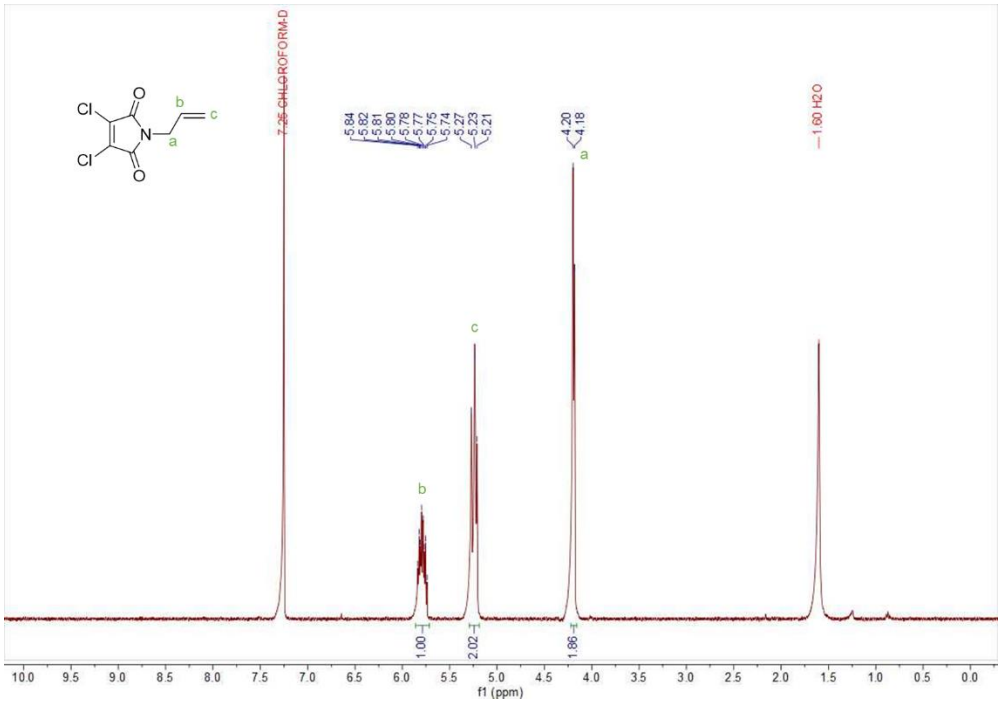

Figure S5. ^{1}H NMR spectrum for compound **DA1**.

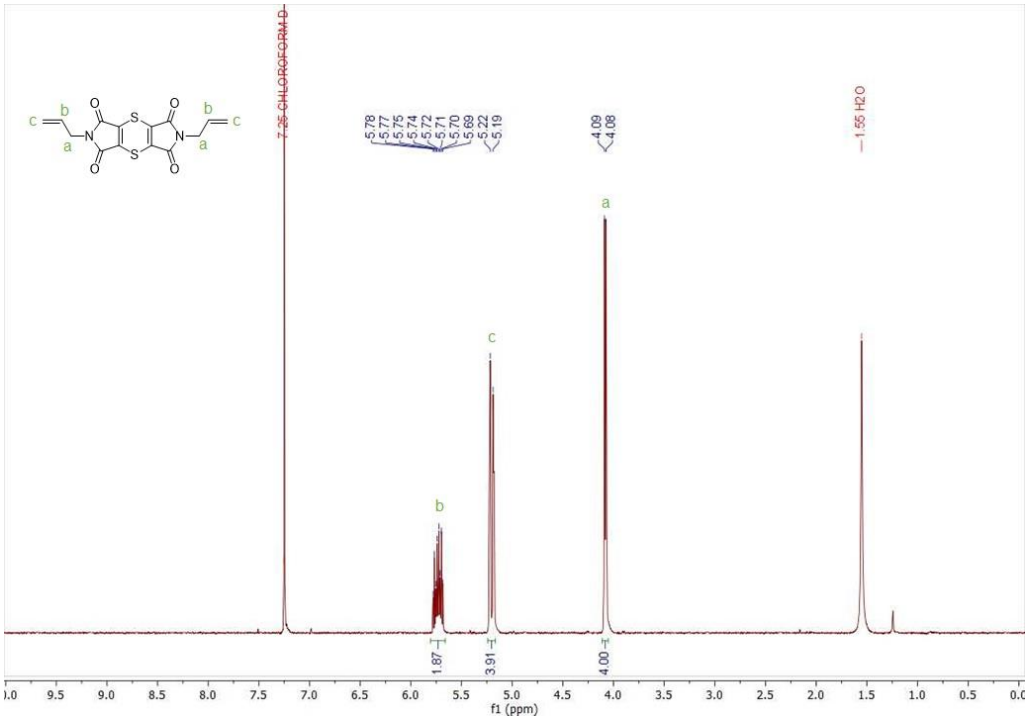

Figure S6. ^{1}H NMR spectrum for compound **DA2**.

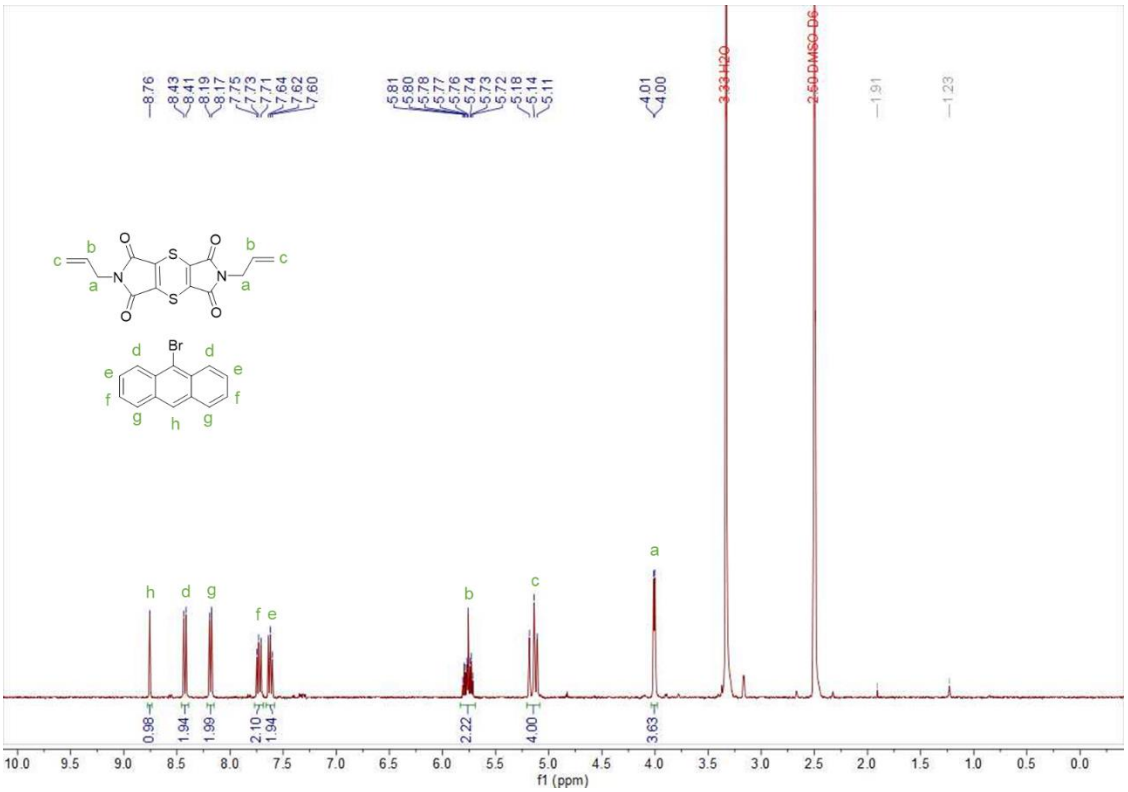

Figure S7. ^{1}H NMR spectrum for **DA2-BrAn**.

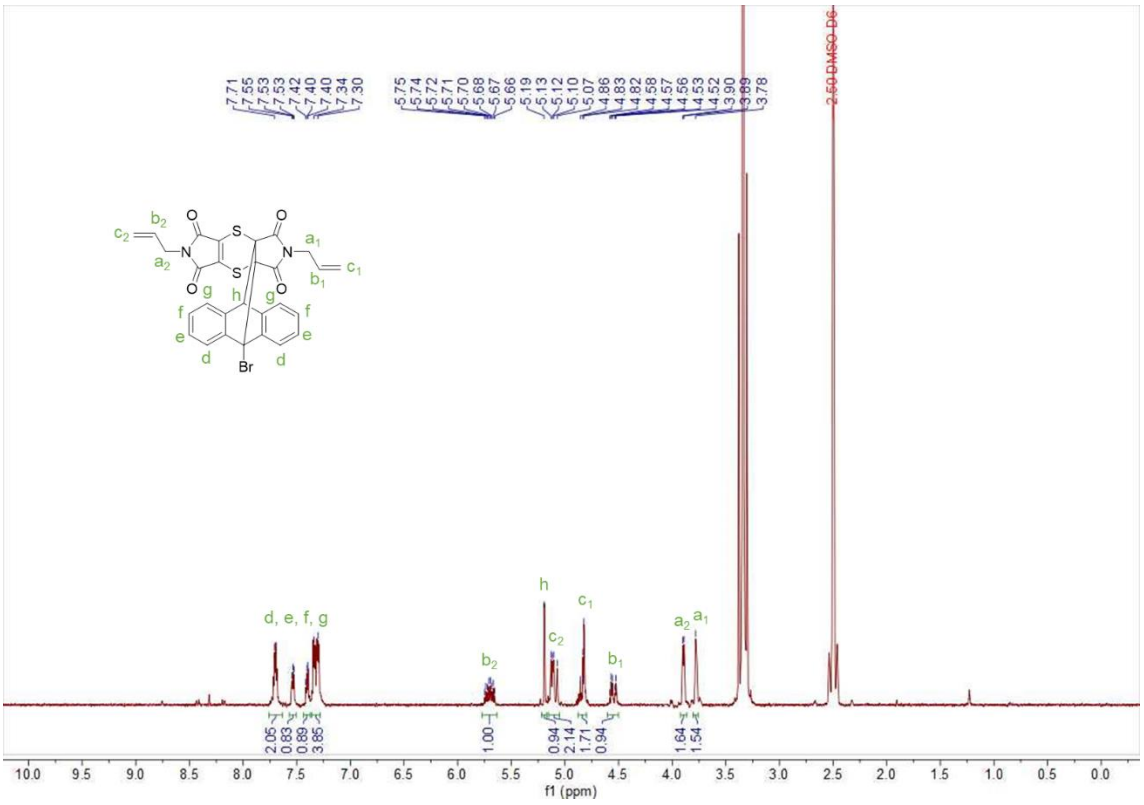

Figure S8. ^{1}H NMR spectrum for **DA2-BrAn CA Nonsolvate**.

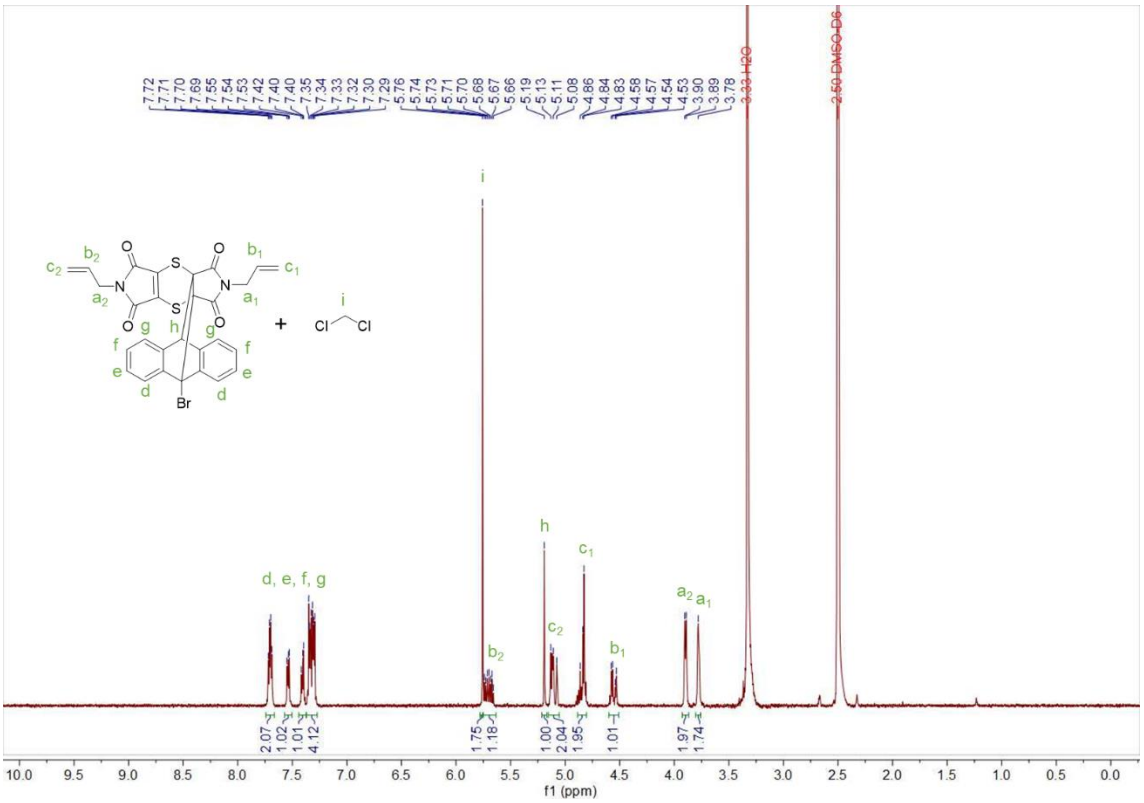

Figure S9. ^{1}H NMR spectrum for compound **DA2-BrAn CA Solvate**.

6. Optical Microscope Images of Crystals

Optical images were collected on a Leica DM2700 M microscope equipped with a Leica MC170 HD microscope camera.

Figure S10. Optical microscope image of **DA2-BrAn H-T** crystals.

Figure S11. Optical microscope image of **DA2-BrAn H-H** crystals.

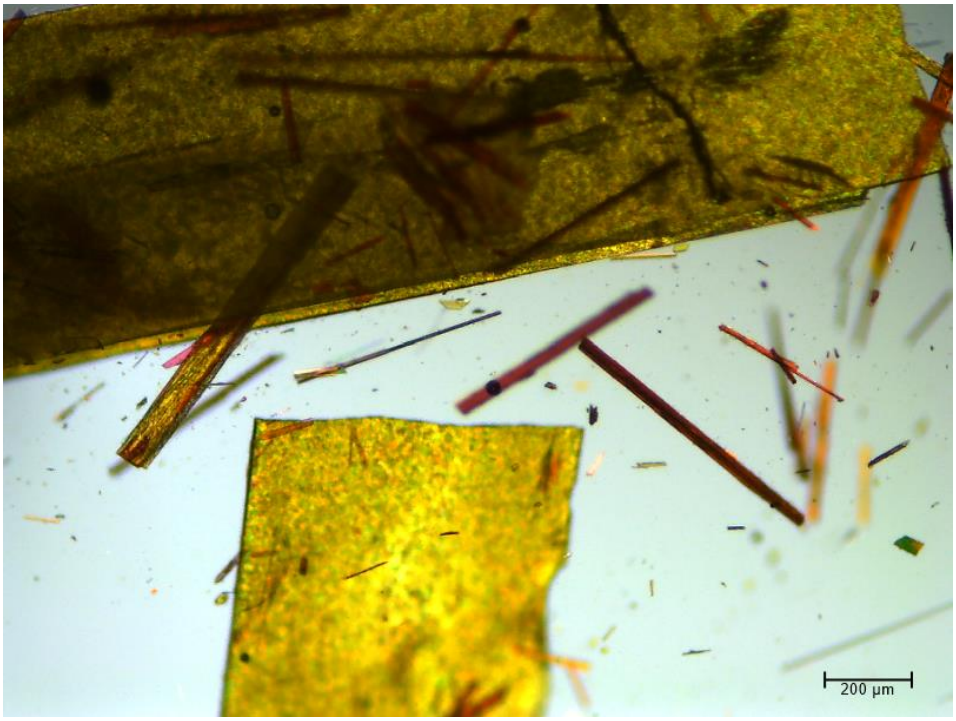

Figure S12. Optical microscope image of **DA2-BrAn H-T CA** crystals (yellow plates) before recrystallization, along with a couple of unreacted H-H cocrystals (needles).

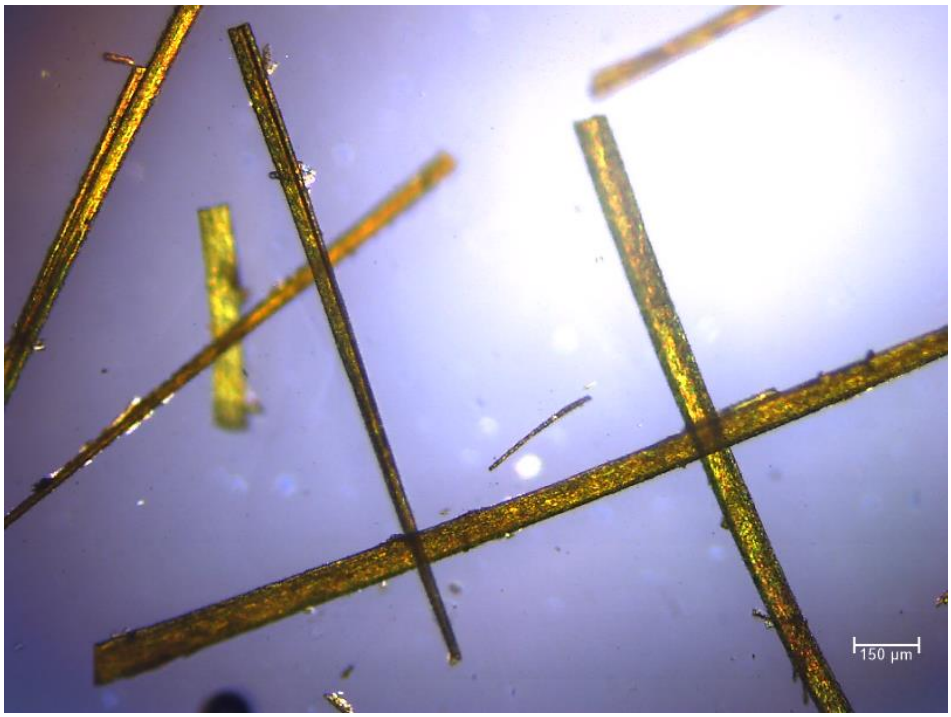

Figure S13. Optical microscope image of **DA2-BrAn H-H CA** crystals before recrystallization.

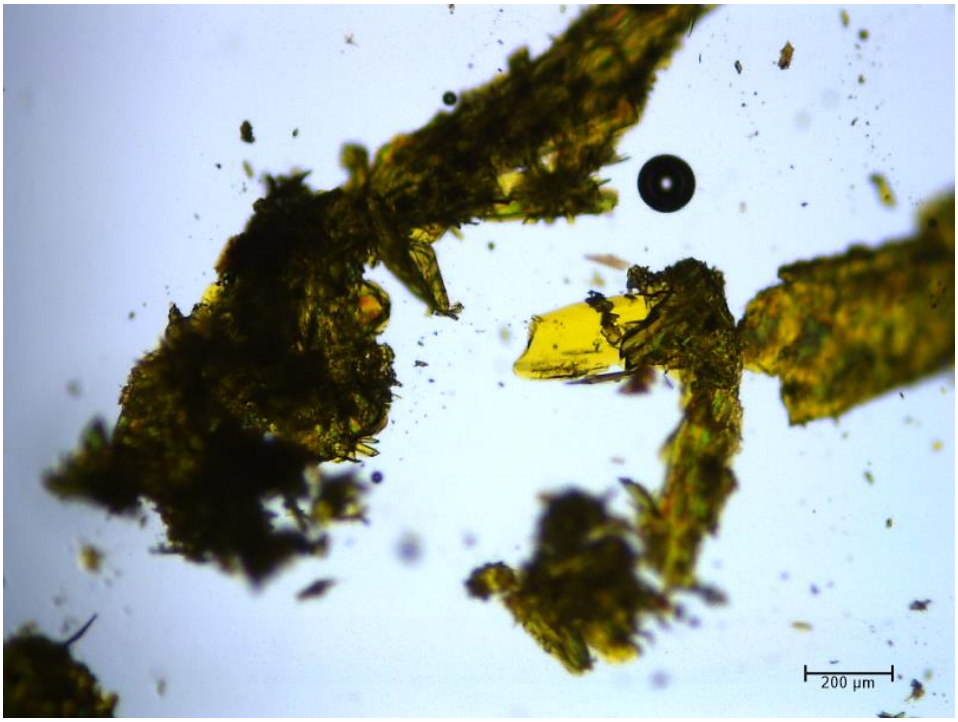

Figure S14. Optical microscope image of **DA2-BrAn CA non-solvate** crystals.

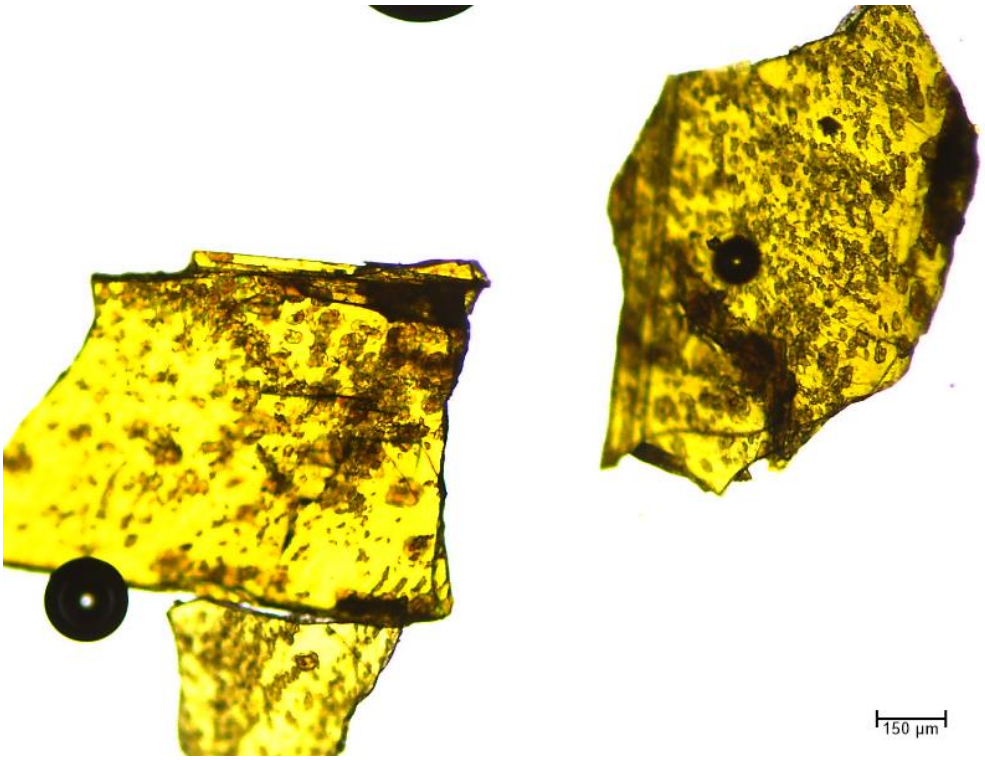

Figure S15. Optical microscope image of **DA2-BrAn CA solvate** crystals.

7. PXRD Patterns

The diffraction patterns for all samples were collected on a Rigaku MiniFlex II powder diffractometer operating in the Bragg-Brentano geometry. An X-ray diffraction pattern was obtained by scanning a 2θ range of 3-60°, step size = 0.02°, and scan time of 2°/minute. The X-ray source was Cu Kα radiation (λ =1.5418 Å) with an anode voltage of 30 kV and a current of 15 mA. Diffraction intensities were recorded on a position sensitive detector (D/teX Ultra). The sample was prepared as a standard powder mount. All semi-quantitative weight percentages were calculated using the whole-pattern fitting software contained within MDI JADE 2022 using the structures with CCDC numbers 2179705 (H-H 300 K) and 2179716 (H-T 300 K) as references.

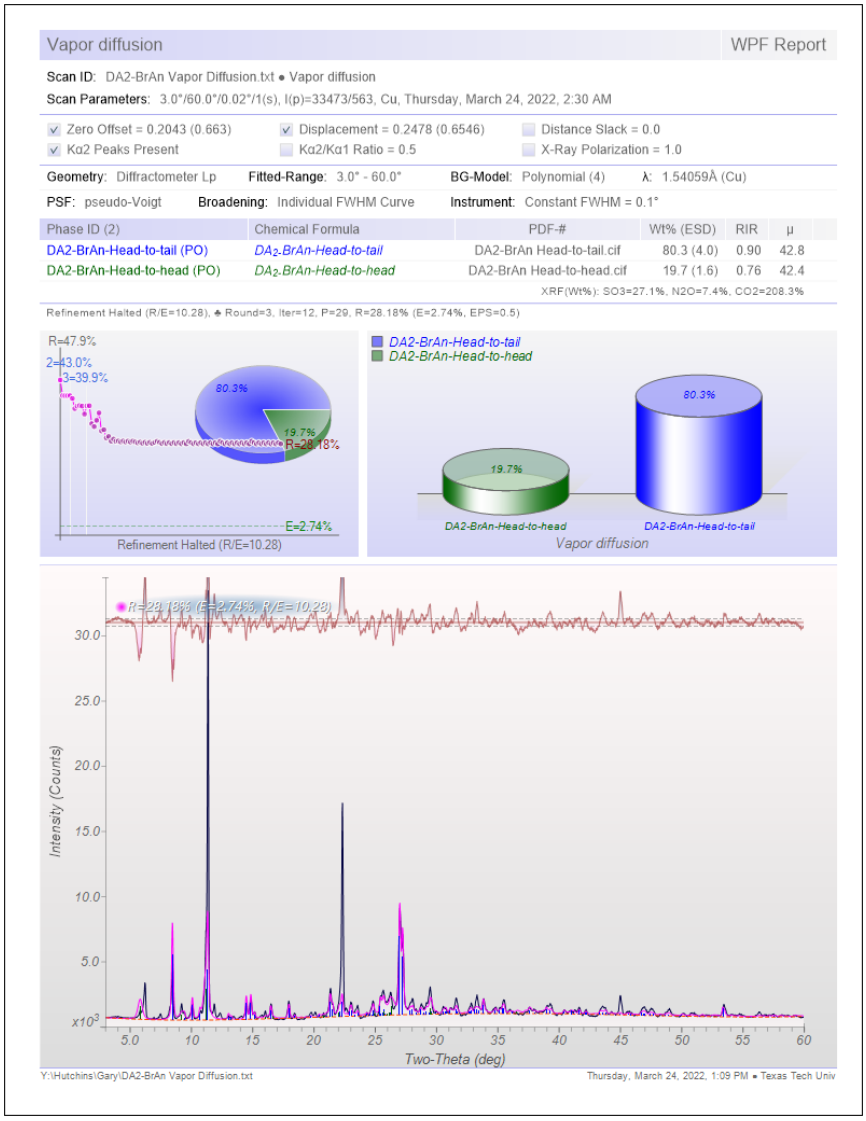

Figure S16. PXRD whole pattern fitting analysis for **DA2-BrAn** from vapor diffusion experiment.

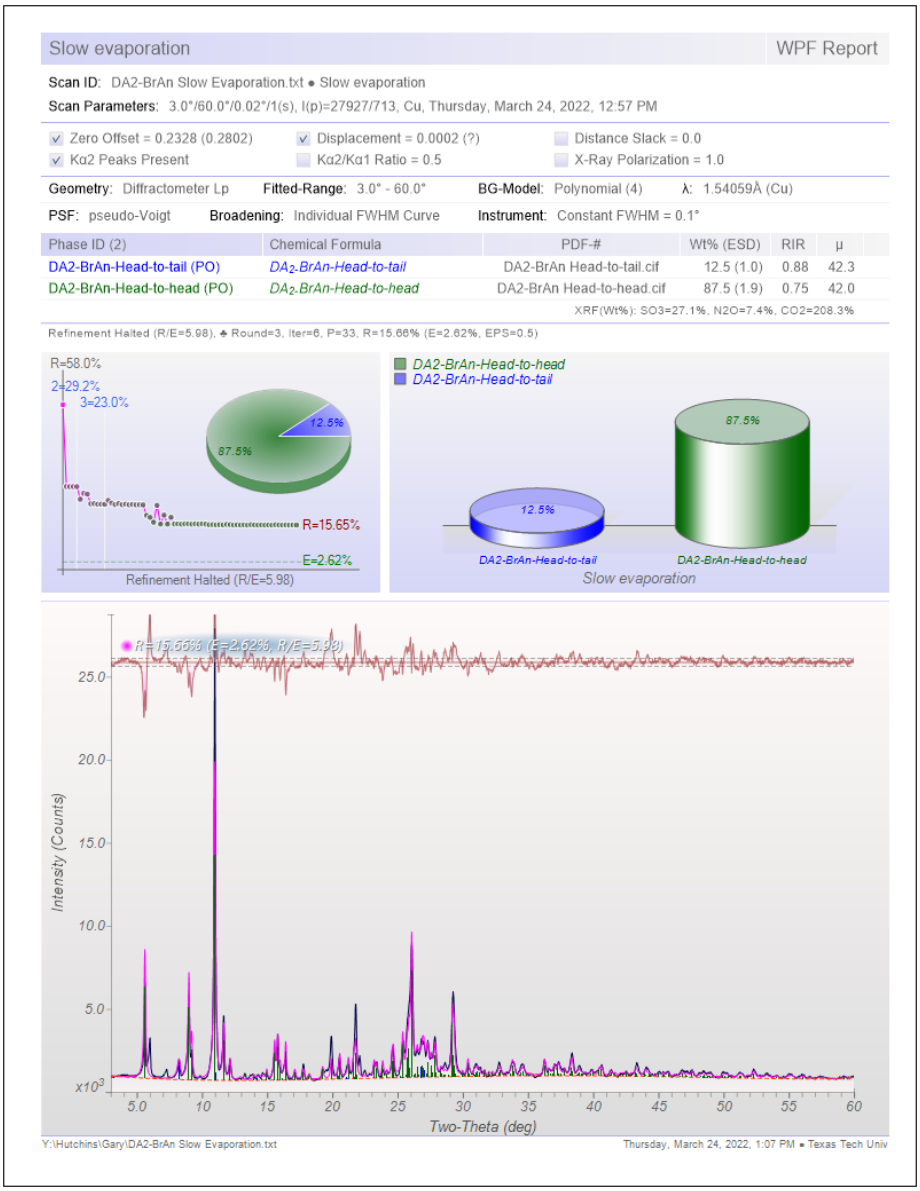

Figure S17. PXRD whole pattern fitting analysis for **DA2-BrAn** from slow evaporation experiment.

8. Variation of the Unit Cell Parameters

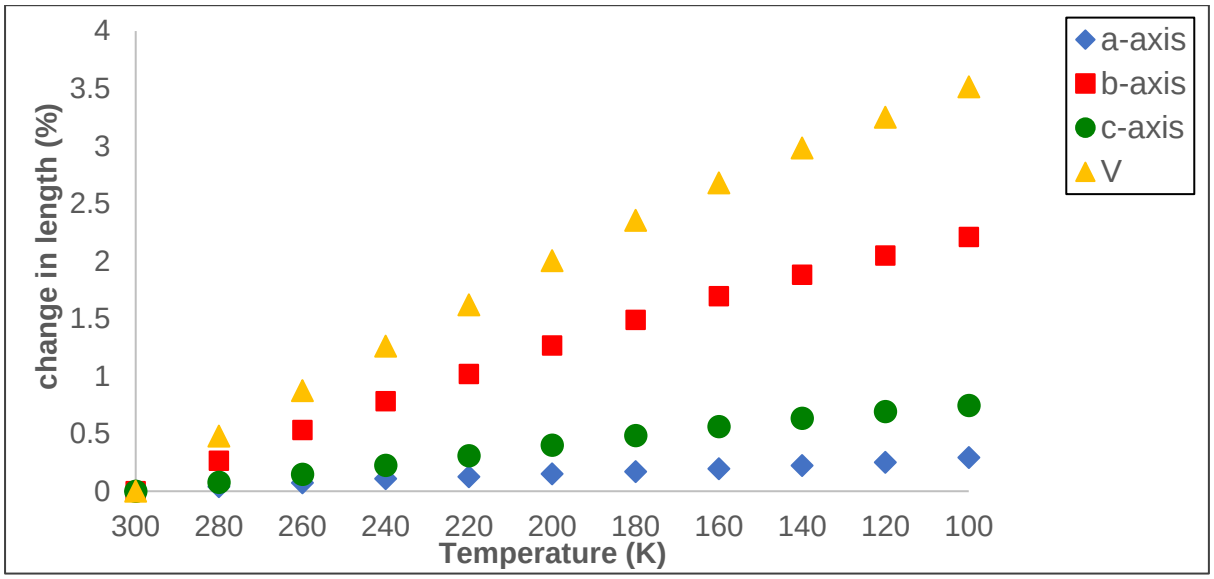

Figure S18. Percent change in length as a function of temperature for **DA2-BrAn H-T**.

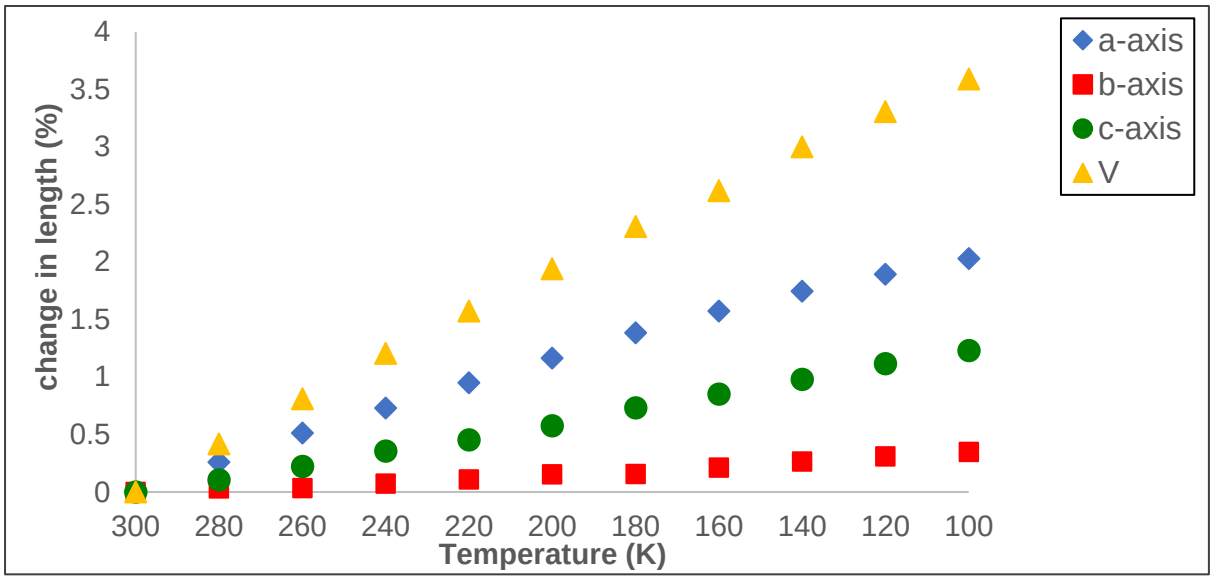

Figure S19. Percent change in length as a function of temperature for **DA2-BrAn H-H**.

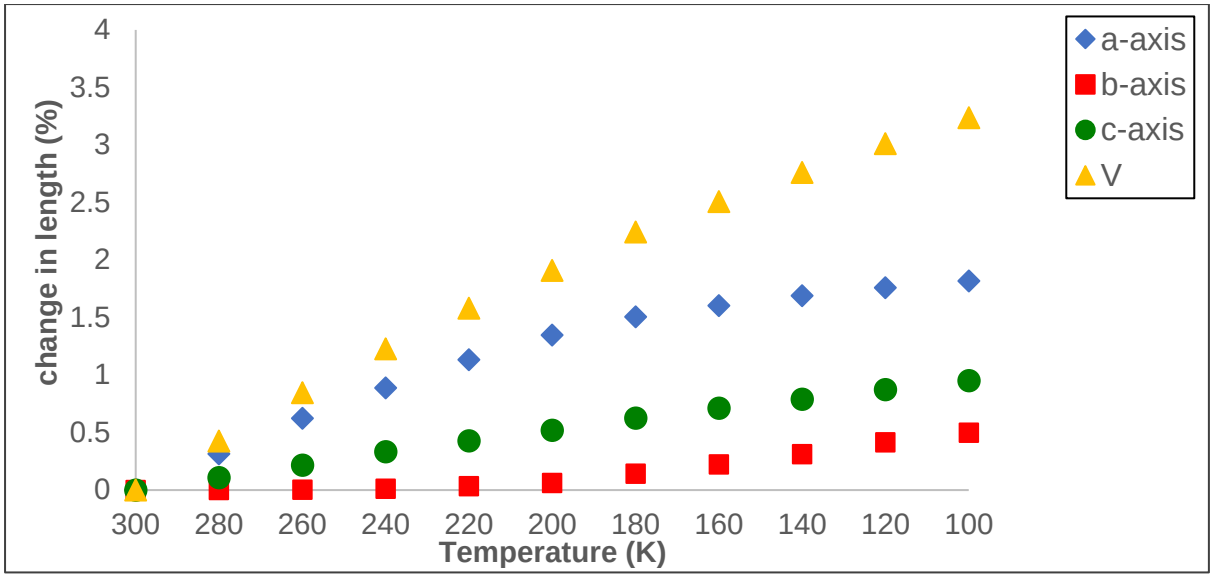

Figure S20. Percent change in length as a function of temperature for **DA2-BrAn CA Nonsolvate**.

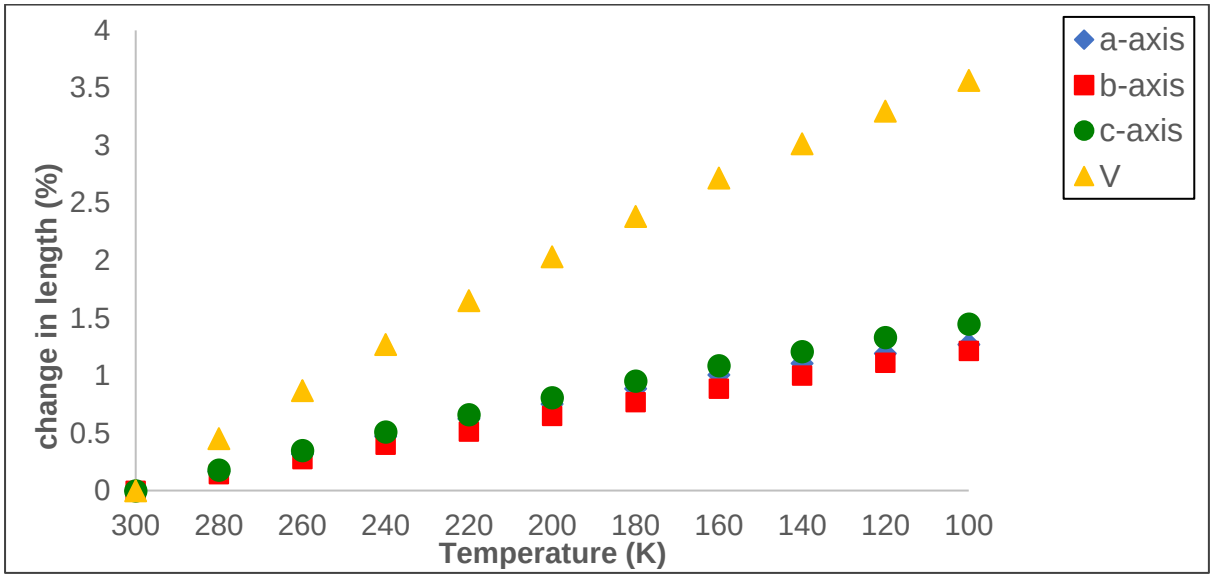

Figure S21. Percent change in length as a function of temperature for **DA2-BrAn CA Solvate**. The *a*-axis symbols are under the *b*- and *c*- axis symbols.

9. Additional Figures

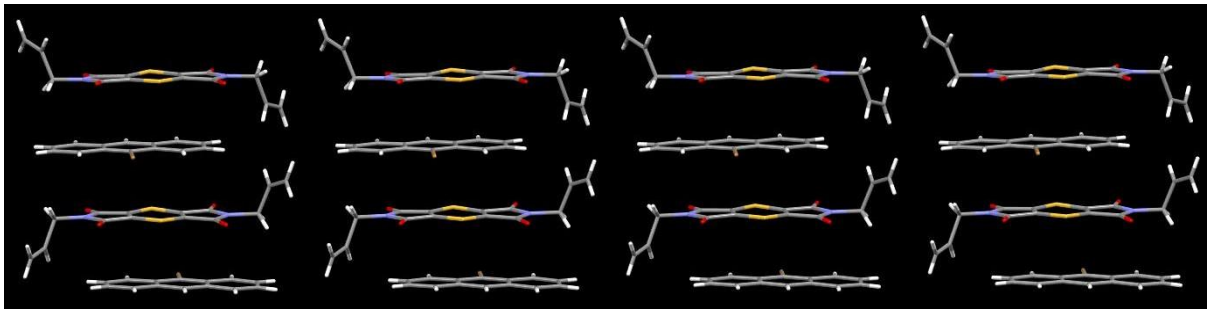

Figure S22. Expanded crystal packing of **DA2-BrAn H-T** cocrystal highlighting the arrangement of neighboring stacks.

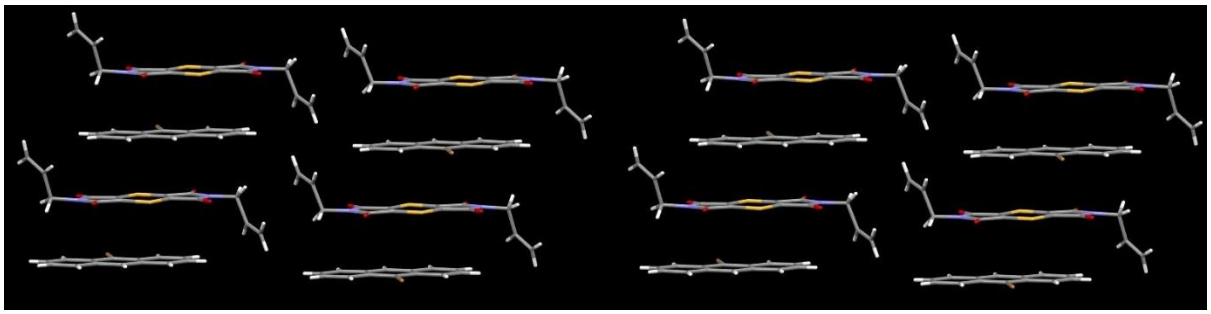

Figure S23. Expanded crystal packing of **DA2-BrAn H-H** cocrystal highlighting the arrangement of neighboring stacks.

10. Variable-Temperature Stage Images

A Leica DM2700 M microscope equipped with a Leica MC170 HD microscope camera was used to collect images during a variable-temperature experiment. A Linkam LTS420 heating/cooling stage equipped with a Linkam T96 Controller and liquid nitrogen cooling system was used to house the crystals during the experiment and control the temperature. Crystals were placed on a glass slide in a minimal amount of type NVH immersion oil by Cargille to keep them in place during the experiment.

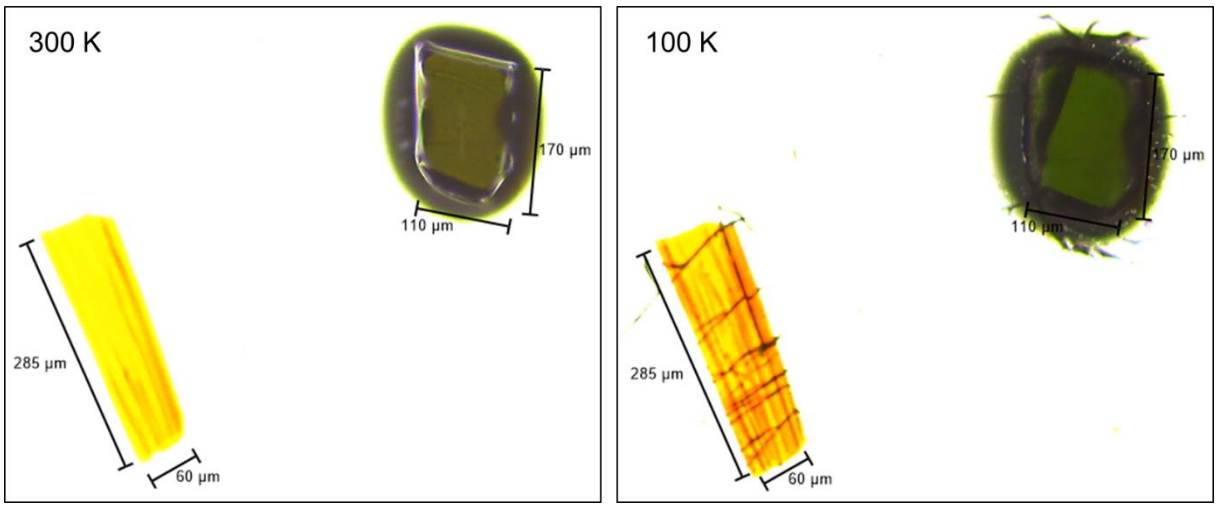

Figure S24. Images of **DA2-BrAn H-H** and **H-T** cocrystals upon warming to 300 K and cooling to 100 K.

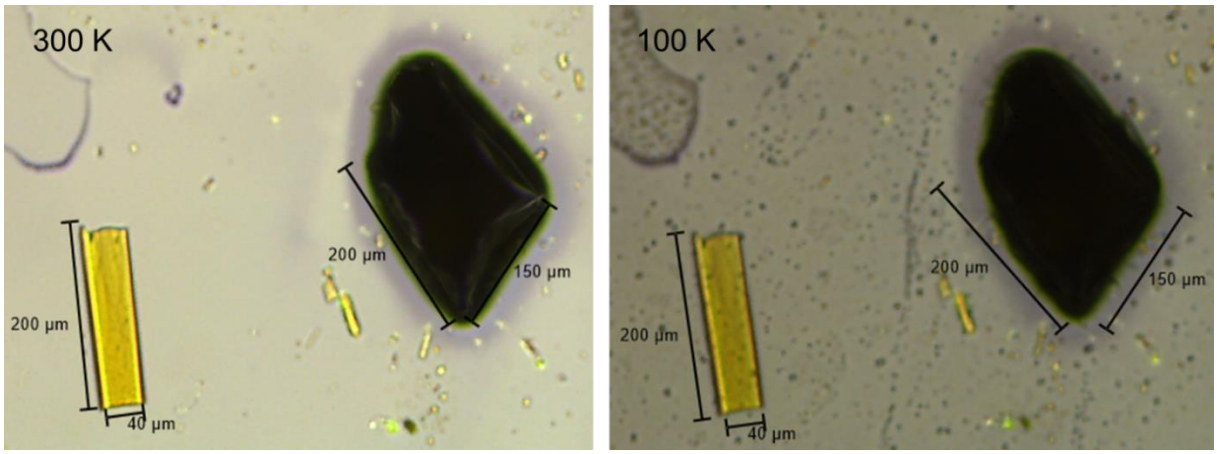

Figure S25. Images of **DA2-BrAn CAs** (before recrystallization) upon warming to 300 K and cooling to 100 K.

11. References

1. Khorasani, S.; Botes, D. S.; Fernandes, M. A.; Levendis, D. C., *CrystEngComm* **2015**, *17*, 8933-8945.

2. CrysAlis^{Pro} (2018) Oxford Diffraction Ltd.

3. SCALE3 ABSPACK (2005) Oxford Diffraction Ltd.

4. Sheldrick, G. M. SHELXT - Integrated space-group and crystal-structure determination. *Acta Crystallogr., Sect. A: Found. Adv.* **2015**, *A71*, 3-8.

5. Sheldrick, G. M. Crystal structure refinement with SHELXL. *Acta. Cryst*. **2015**, *71*, 3-8.

6. Dolomanov, O. V.; Bourhis, L. J.; Gildea, R. J.; Howard, J. A. K.; Puschmann. H. OLEX2: a complete structure solution, refinement and analysis program. *J. Appl. Cryst*. **2009**, *42*, 339-341.

7. Cliffe, M. J.; Goodwin, A. L. *J. Appl. Cryst*. **2012**, *45*, 1321-1329.